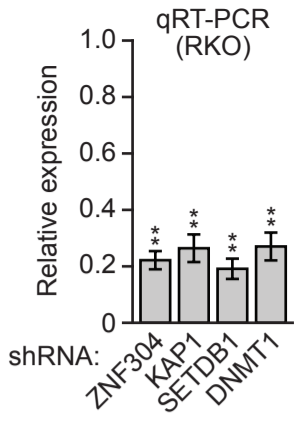
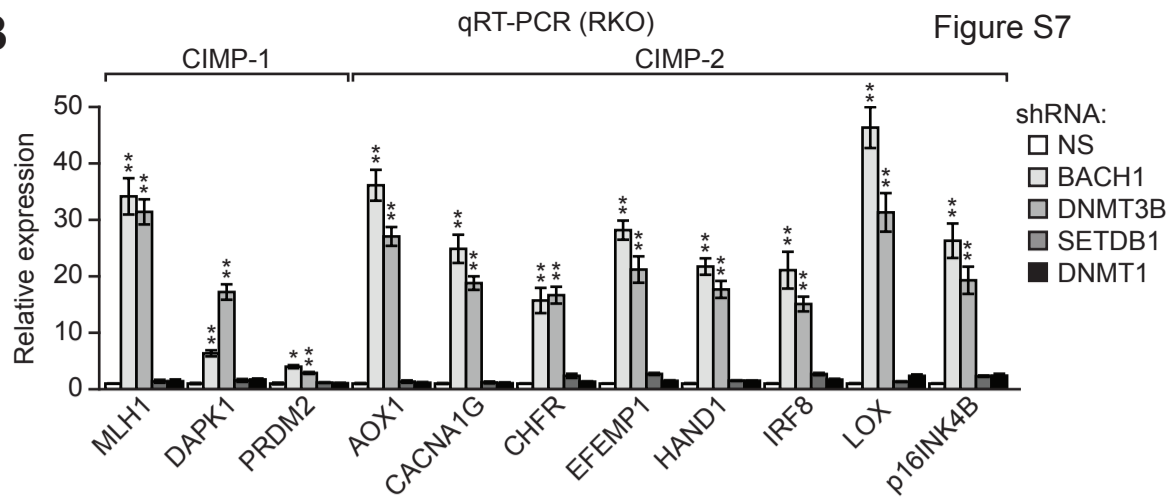
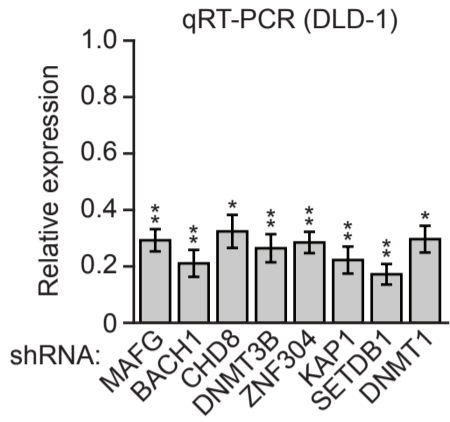
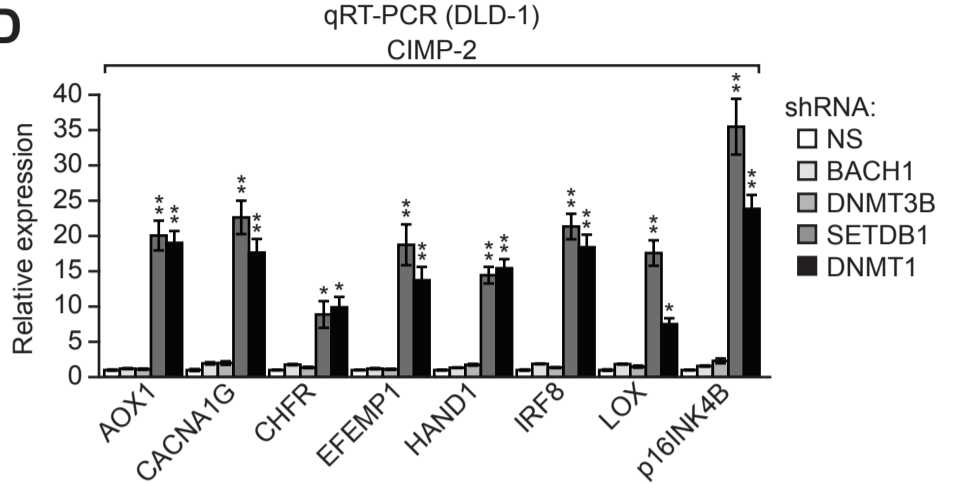
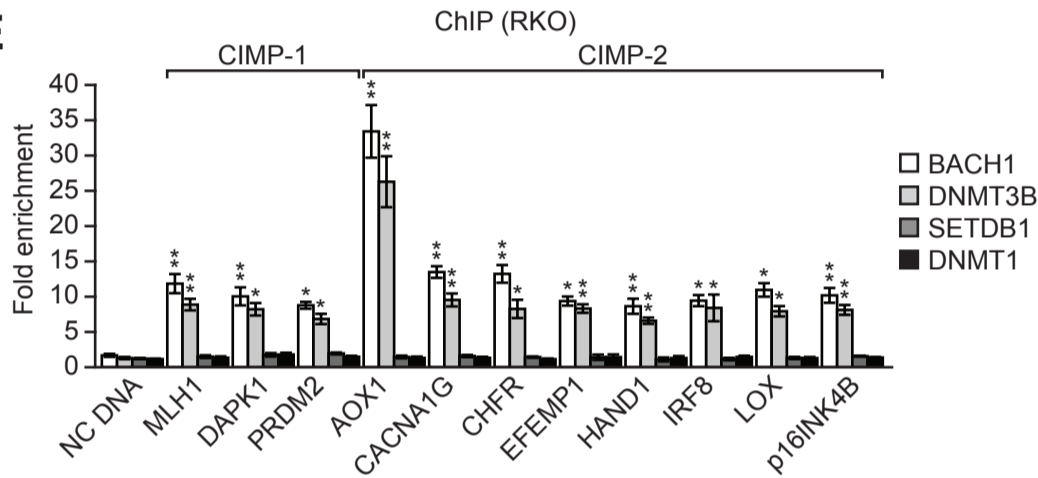
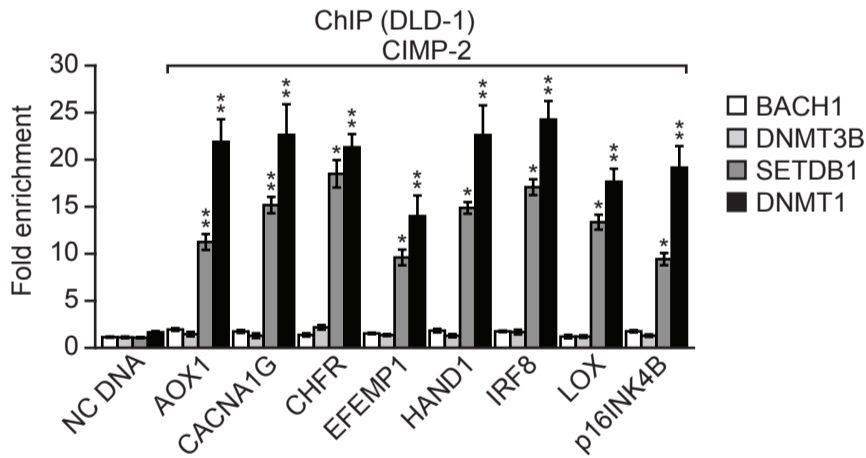
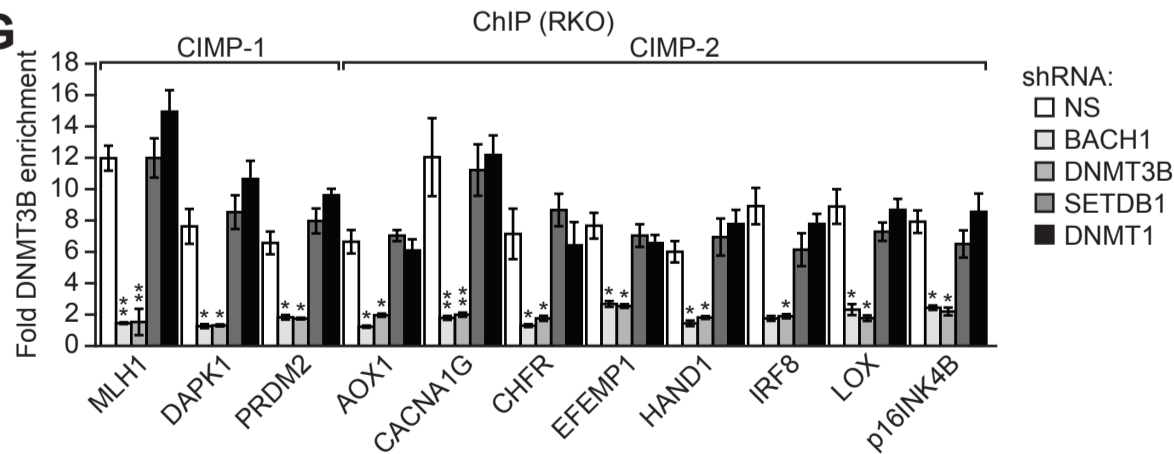
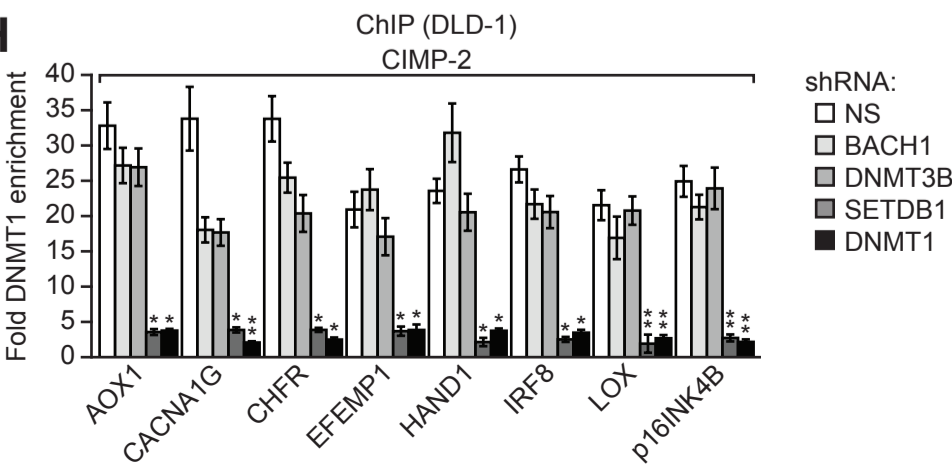


**A****B****C****D****E****F****G****H**

## Supplemental Figure Legends

### Figure S1. Validation of Candidates from the RNAi Screen for a Role in *MLH1* Transcriptional Silencing in RKO Cells (Related to Figure 1)

(A) qRT-PCR analysis monitoring expression of *MLH1* in RKO cells expressing a second shRNA targeting one of the 16 candidate genes that was unrelated to that isolated in the primary shRNA screen.

(B and C) qRT-PCR analysis monitoring shRNA-mediated knockdown efficiency for each candidate gene using an shRNA isolated from the primary screen (B) as well as a second, unrelated shRNA against the same target gene (C). Data are represented as mean  $\pm$  SD. \* $P \leq 0.05$ , \*\* $P \leq 0.01$ .

### Figure S2. Experiments Related to Figure 2

(A) ChIP analysis monitoring occupancy of MAFG and other candidate transcriptional repressors isolated from the RNAi screen at the -500 bp region of the *MLH1* promoter (see panel F below).

(B) OncoPrint box plot analysis showing that *MAFG* is over-expressed in colorectal cancers. The study analyzed 100 colorectal carcinoma and 5 normal colon samples (Kaiser et al., 2007) as follows: 0, Normal colon (5); 1, Cecum adenocarcinoma (17); 2, Colon adenocarcinoma (41); 3, Colon mucinous adenocarcinoma (13); 4, Colon signet ring cell adenocarcinoma (2); 5, Colon small cell carcinoma (2); 6, Rectal adenocarcinoma (8); 7, Rectal mucinous adenocarcinoma (4); 8, Rectal signet ring cell adenocarcinoma (1); 9, Rectosigmoid adenocarcinoma (10); 10, Rectosigmoid mucinous adenocarcinoma (2).

(C) qRT-PCR analysis monitoring *MLH1* expression in RKO cells expressing a second shRNA targeting candidate MAFG corepressors that is unrelated to that used in Figures 2A and 2B.



(D) qRT-PCR analysis monitoring shRNA-mediated knockdown efficiency for each candidate corepressor using two unrelated shRNAs against the same target gene.

(E) Bisulfite sequencing analysis of the *MINT6* promoter in RKO cells expressing a NS, MAFG, BACH1, CHD8 or DNMT3B shRNA. Decreased promoter hypermethylation in the presence of 5-AZA is shown as a control. (Top) Schematic of the *MINT6* promoter; positions of CpGs are shown to scale by vertical lines. (Bottom) Each circle represents a methylated (black) or unmethylated (white) CpG dinucleotide. Each row represents a single clone.

(F) ChIP analysis monitoring occupancy of MAFG, BACH1, CHD8 and DNMT3B at various regions within ~5 kb of the *MLH1* promoter and 5' UTR in RKO cells. The locations of the primer pairs used for the ChIP analysis are indicated. Binding at the -500 bp region of the *MLH1* promoter was chosen for all ChIP experiments. Data are represented as mean  $\pm$  SD. \* $P \leq 0.05$ , \*\* $P \leq 0.01$ .

(G) Co-immunoprecipitation analysis. RKO cell extracts were immunoprecipitated with a DNMT1, MAFG or control (IgG) antibody, and the immunoprecipitate was analyzed for DNMT1 and MAFG by immunoblotting.

(H) Selected results from the mass spectroscopy analysis listing proteins with a known function in transcriptional silencing or other transcriptional regulators, and their total spectra score (TSC) in samples immunoprecipitated using either IgG or a MAFG antibody. BACH1, CHD8 and DNMT3B, the proteins shown to interact with MAFG by co-immunoprecipitation, are highlighted in yellow. The probability of interaction, derived from the Scaffold Viewer software is shown; purple indicates an 80-94% probability of interaction, and green indicates a  $\geq 95\%$  probability of interaction.

### **Figure S3. Experiments Related to Figure 3**

(A) qRT-PCR analysis monitoring knockdown efficiency of BRAF in RKO cells expressing a NS shRNA or a second BRAF shRNA unrelated to that used in Figure 3C.

(B) qRT-PCR analysis monitoring *MLH1* expression in RKO cells expressing a NS shRNA or one of two unrelated BRAF shRNAs.

(C) Immunoblot analysis monitoring the levels of MAFG and its corepressors in RKO cells treated with DMSO or with 1  $\mu$ M PLX4720 or U0126 for 24 hours. Phosphorylated ERK1/2 (p-ERK1/2) and total ERK1/2 (t-ERK1/2) were monitored as controls.  $\alpha$ -tubulin (TUBA) was monitored as a loading control.

(D) Immunoblot analysis monitoring the levels of MAFG in PFFs and RKO cells.

(E) Co-immunoprecipitation analysis. PFF cell extracts were immunoprecipitated with a MAFG, BACH1, CHD8, DNMT3B or control (IgG) antibody, and the immunoprecipitate was analyzed for MAFG, BACH1, CHD8 or DNMT3B by immunoblotting.

(F) ChIP analysis monitoring binding of MAFG, BACH1, CHD8 and DNMT3B to the *MLH1* promoter (at the -500 bp region) in PFFs. The results were normalized to that obtained with IgG, which was set to 1.

(G) qRT-PCR analysis monitoring *MLH1* expression in PFFs expressing a NS shRNA or one of two unrelated MAFG shRNAs. Data are represented as mean  $\pm$  SD. \* $P \leq 0.05$ , \*\* $P \leq 0.01$ .

(H) Multiple sequence alignment showing conservation of the two putative ERK consensus phosphorylation sites in MAFG. The alignment was performed using NCBI's HomoloGene using *H. sapiens* (NP\_002350.1), *P. troglodytes* (XP\_001166122.1), *M. mulatta* (XP\_001112718.1), *C. lupus* (XP\_849862.2), *B. taurus* (NP\_001092450.1), *M. musculus* (NP\_034886.1), *R. norvegicus* (NP\_071781.1), *G. gallus* (NP\_001072957.1) and *D. rerio* (NP\_001002045.1) sequences. Amino acid numbers refer to the human protein.

(I) Immunoblot analysis monitoring the levels of MAFG and FBXW2 in RKO cells expressing a NS shRNA or one of two unrelated FBXW2 shRNAs.

**Figure S4. The *MLH1* Promoter is Hypermethylated in BRAF-Positive Human CRC Tumor Samples but not in Matched Normal Controls (Related to Figure 4)**

Bisulfite sequencing analysis of the *MLH1* promoter in matched adjacent normal (N) and BRAF-positive CRC human tumor (T) samples. (Top) Schematic of the *MLH1* promoter; positions of CpGs are shown to scale by vertical lines. (Bottom) Each circle represents a methylated (black) or unmethylated (white) CpG dinucleotide. Each row represents a single clone.

**Figure S5. Confirmation of CIMP-Positive Status of RKO Cells, and Expression Analysis of Representative Non-CIMP genes Upon Knockdown of MAFG or its Corepressors (Related to Figure 5)**

(A) Bisulfite sequencing analysis of the *MLH1*, *DAPK*, *p14ARF* and *IRF8* promoters in RKO cells. (Top) Schematic of the promoters; positions of CpGs are shown to scale by vertical lines. (Bottom) Each circle represents a methylated (black) or unmethylated (white) CpG dinucleotide. Each row represents a single clone. The results show that the CIMP gene promoters are hypermethylated, confirming the cell lines are CIMP-positive.

(B) qRT-PCR analysis monitoring expression of *VIM* and *SEPT9* in RKO cells expressing a NS, BACH1, CHD8 or DNMT3B shRNA.

(C) qRT-PCR analysis monitoring expression of representative hypermethylated non-CIMP genes that flank *MLH1* in RKO cells expressing a NS, BACH1, CHD8 or DNMT3B shRNA.

(D) qRT-PCR analysis monitoring expression of representative CIMP genes in RKO cells expressing a NS, MAFG, BACH, CHD8 or DNMT3B shRNA. Data are represented as mean  $\pm$  SD. \* $P \leq 0.05$ , \*\* $P \leq 0.01$ .

**Figure S6. Experiments Related to Figure 6**

(A) Bisulfite sequencing analysis of the *MLH1*, *DAPK*, *p14ARF* and *IRF8* promoters in VACO432 and SW48 cells. (Top) Schematic of the promoters; positions of CpGs are shown to scale by vertical lines. (Bottom) Each circle represents a methylated (black) or unmethylated

(white) CpG dinucleotide. Each row represents a single clone. The results show that the CIMP gene promoters are hypermethylated, confirming the cell lines are CIMP-positive.

(B) Bisulfite sequencing analysis of the *DAPK*, *p14ARF* and *IRF8* promoters in matched adjacent normal (N) and BRAF-positive CRC human tumor (T) samples.

(C) qRT-PCR analysis monitoring expression of CIMP genes in RKO cells expressing a BRAF shRNA or treated with 1  $\mu$ M PLX4720. The results were normalized to that observed upon expression of a NS shRNA or upon DMSO treatment, which were set to 1.

(D) qRT-PCR analysis monitoring expression of representative CIMP genes in VACO432 cells treated with DMSO, or 1  $\mu$ M PLX4720 or U0126 for 24 hours.

(E) qRT-PCR analysis monitoring expression of representative CIMP genes in SW48 cells treated with DMSO, or 1  $\mu$ M gefitinib or U0126 for 24 hours.

(F) qRT-PCR analysis monitoring expression of representative CIMP genes in RKO cells treated with DMSO or 1  $\mu$ M U0126 for 24 hours. Data are represented as mean  $\pm$  SD. \* $P \leq 0.05$ , \*\* $P \leq 0.01$ .

**Figure S7. Oncogenic BRAF and KRAS Direct the Assembly of Distinct Repressor Complexes on Common CIMP Gene Promoters (Related to Figure 7)**

(A) qRT-PCR analysis monitoring shRNA-mediated knockdown efficiency of ZNF304, KAP1, SETB1 and DNMT1 in RKO cells.

(B) qRT-PCR analysis monitoring CIMP gene expression in RKO cells expressing a NS, BACH1, DNMT3B, SETDB1 or DNMT1 shRNA.

(C) qRT-PCR analysis monitoring shRNA-mediated knockdown efficiency of MAFG, BACH1, CHD8 and DNMT3B in DLD-1 cells.

(D) qRT-PCR analysis monitoring CIMP gene expression in DLD-1 cells expressing a NS, BACH1, DNMT3B, SETDB1 or DNMT1 shRNA.

(E and F) ChIP analysis monitoring binding of BACH1, DNMT3B, SETDB1 and DNMT1 on CIMP gene promoters in RKO (E) and DLD-1 (F) cells.

(G and H) ChIP analysis monitoring binding of DNMT3B to CIMP gene promoters in RKO cells (G) and binding of DNMT1 to CIMP gene promoters in DLD-1 cells (H) expressing a NS, BACH1, DNMT3B, SETDB1 or DNMT1 shRNA.

**Table S1. List of Candidate Genes Obtained from the Primary Screen that Validate with Two Independent shRNAs (Related to Figure 1)**

<b>Biological process</b>	<b>Gene symbol</b>	<b>Gene name</b>
Transcription	<i>CHD8</i>	chromodomain helicase DNA binding protein 8
	<i>ING1</i>	inhibitor of growth family, member 1
	<i>MAFG</i>	v-maf avian musculoaponeurotic fibrosarcoma oncogene homolog G
	<i>MAML3</i>	mastermind-like 3 (Drosophila)
	<i>TARBP1</i>	TAR (HIV-1) RNA binding protein 1
	<i>ZBED5</i>	zinc finger, BED-type containing 5
	<i>ZFHX2</i>	zinc finger homeobox 2
	<i>ZFYVE27</i>	zinc finger, FYVE domain containing 27
	<i>ZNF701</i>	zinc finger protein 701
Chromatin structure	<i>HIST2H2AA3</i>	histone cluster 2, H2aa3
Translation	<i>EIF2S1</i>	eukaryotic translation initiation factor 2, subunit 1 alpha, 35kDa
Protein folding/stability	<i>DNAJB12</i>	DnaJ (Hsp40) homolog, subfamily B, member 12
	<i>FBXW2</i>	F-box and WD repeat domain containing 2
Cell growth arrest/apoptosis	<i>VWA5A</i>	von Willebrand factor A domain containing 5A
Cell signaling	<i>MAPK9</i>	mitogen-activated protein kinase 9
	<i>STYX</i>	serine/threonine/tyrosine interacting protein

**Table S2. Mass Spectrometry Analysis of Proteins that Interact with MAFG (Related to Figure 2).**

See the accompanying Excel file.

**Table S3. Identification of MAFG Consensus Binding Sites in the Promoters of CIMP Genes (Related to Figure 5).** MAFG heterodimeric complexes bind to the consensus sequence TGCTGA(G/C)TCAGCA (which contains a “core” sequence of TGA[G/C]TCA) or TGCTGA(GC/CG)TCAGCA (which contains a core sequence TGA[GC/CG]TCA) (Kataoka et al., 1994). To identify MAFG consensus binding sites in CIMP promoters, we scanned a region from 5 kb upstream of the transcription start site through the 5' untranslated region, and allowed up to one mismatch in the core and four mismatches in total, which is permissible to retain MAFG binding (Kataoka et al., 1994).

See the accompanying Excel file.



**Table S4. List of Catalog Numbers for shRNAs Obtained from Open Biosystems/Thermo Scientific (Related to Experimental Procedures)**

<b>Gene</b>	<b>1<sup>st</sup> shRNA</b>	<b>2<sup>nd</sup> shRNA</b>
<i>BACH1</i>	TRCN0000013536	TRCN0000013533
<i>BACH2</i>	TRCN0000018114	TRCN0000018116
<i>BRAF</i>	TRCN0000006292	TRCN0000006290
<i>CHD8</i>	TRCN0000016509	TRCN0000016512
<i>DNAJB12</i>	TRCN0000022296	TRCN0000022297
<i>DNMT1</i>	V2LHS_113506	V2LHS_113505
<i>DNMT3A</i>	V2LHS_74666	V3LHS_391163
<i>DNMT3B</i>	TRCN0000035687	TRCN0000035686
<i>EIF2S1</i>	TRCN00000159938	TRCN0000035758
<i>FBXW2</i>	TRCN0000006547	TRCN0000006549
<i>HIST2H2AA3</i>	TRCN0000074590	TRCN0000074592
<i>ING1</i>	TRCN0000073268	TRCN0000073271
<i>KAP1</i>	TRCN0000018002	TRCN0000017998
<i>MAML3</i>	TRCN0000063893	TRCN0000063896
<i>MAFG</i>	TRCN0000015190	TRCN0000015191
<i>MAPK9</i>	TRCN0000010277	TRCN0000010278
<i>NFE2L1</i>	TRCN0000014623	TRCN0000014626
<i>SETDB1</i>	V3LHS_388251	V3LHS_388253
<i>STYX</i>	TRCN0000006899	TRCN0000006898
<i>TARBP1</i>	TRCN0000021820	TRCN0000021822
<i>VWA5A</i>	TRCN00000128376	TRCN0000021823
<i>ZBED5</i>	TRCN00000158509	TRCN0000021825
<i>ZFH2</i>	TRCN0000016653	TRCN0000016655
<i>ZFYVE27</i>	TRCN00000136870	TRCN0000016657
<i>ZNF701</i>	TRCN0000020885	TRCN0000020886
<i>ZNF304</i>	TRCN00000108038	TRCN00000108037

**Table S5. List of Primers used for qRT-PCR, ChIP, PAT-ChIP, Bisulfite Sequencing and Cloning (Related to Experimental Procedures)**

See the accompanying Excel file.

## Supplemental Experimental Procedures

### Liquid Chromatography Tandem Mass Spectrometry

Large-scale immunoprecipitation was performed in RKO cell extracts using a MAFG antibody (Santa Cruz) as previously described (Wang et al., 2000), except Protein A sepharose beads were replaced by Protein G DynaBeads (Invitrogen). The precipitated proteins were eluted with Laemmli sample buffer and separated on a short 10% SDS-polyacrylamide gel. A 2 cm gel slice with all the proteins was submitted for mass spectrometry at the University of Massachusetts Medical School Proteomics and Mass Spectrometry Facility.

Gel slices were cut into 1x1 mm pieces and placed in 1.5 ml eppendorf tubes with 1 ml of water for 30 min. The water was removed and 100  $\mu$ l of 250 mM ammonium bicarbonate was added. For reduction, 20  $\mu$ l of a 45 mM solution of 1, 4 dithiothreitol (DTT) was added and the samples were incubated at 50°C for 30 min. The samples were cooled to room temperature and then, for alkylation, 20  $\mu$ l of a 100 mM iodoacetamide solution was added and allowed to react for 30 min. The gel slices were washed two times with 1 ml water aliquots. The water was removed and 1 ml of 50:50 (50 mM ammonium bicarbonate: acetonitrile) was placed in each tube and samples were incubated at room temperature for 1 hr. The solution was then removed and 200  $\mu$ l of acetonitrile was added to each tube at which point the gels slices turned opaque white. The acetonitrile was removed and gel slices were further dried in a Speed Vac. Gel slices were rehydrated in 50  $\mu$ l of 2 ng/ $\mu$ l trypsin (Sigma) in 0.01% ProteaseMAX Surfactant (Promega): 50 mM ammonium bicarbonate. Additional bicarbonate buffer was added to ensure complete submersion of the gel slices. Samples were incubated at 37°C for 21 hrs. The supernatant of each sample was then removed and placed in a separate 1.5 ml eppendorf tube. Gel slices were further dehydrated with 100  $\mu$ l of 80:20 (Acetonitrile: 1% formic acid). The extract was combined with the supernatants of each sample. The samples were then dried in a

Speed Vac. Samples were dissolved in 25  $\mu$ l of 5% acetonitrile in 0.1% trifluoroacetic acid prior to injection on LC/MS/MS.

A 4.0  $\mu$ l aliquot was directly injected onto a custom packed 2 cm x 100  $\mu$ m C<sub>18</sub> Magic 5 $\mu$  particle trap column. Labeled peptides were then eluted and sprayed from a custom packed emitter (75  $\mu$ m x 25 cm C<sub>18</sub> Magic 3  $\mu$ m particle) with a linear gradient from 95% solvent A (0.1% formic acid in water) to 35% solvent B (0.1% formic acid in acetonitrile) in 90 min at a flow rate of 300 nl per minute on a Waters Nano Acquity UPLC system. Data dependent acquisitions were performed on a Q Exactive mass spectrometer (Thermo Scientific) according to an experiment where full MS scans from 300-1750 m/z were acquired at a resolution of 70,000 followed by 10 MS/MS scans acquired under HCD fragmentation at a resolution of 17,500 with an isolation width of 1.6 Da. Raw data files were processed with Proteome Discoverer (version 1.3) prior to searching with Mascot Server (version 2.4) against the Human Index of the SwissProt database. Search parameters utilized were fully tryptic with two missed cleavages, parent mass tolerances of 10 ppm and fragment mass tolerances of 0.05 Da. A fixed modification of carbamidomethyl cysteine and variable modifications of acetyl (protein N-term), pyro glutamic for N-term glutamine, oxidation of methionine were considered. Search results were loaded into Scaffold Viewer (Proteome Software, Inc.), which provided total spectra scores (TSC) and interaction probabilities.

### **Identification of MAFG Consensus Binding Sites in CIMP Gene Promoters**

For each CIMP gene, a region from 5 kb upstream of the transcription start site through the 5' untranslated region was extracted from the UCSC human genome (hg19) assembly by R/Bioconductor GenomicFeatures (v1.16.2) package. The consensus searching was done by R (v3.1.0)/Bioconductor (v2.14) Biostrings (v2.32.1) package using a search criteria of 0 or 1 nucleotide mismatch in the core and a total maximum mismatch of 4 nucleotides.

## Supplemental References

Kaiser, S., Park, Y.K., Franklin, J.L., Halberg, R.B., Yu, M., Jessen, W.J., Freudenberg, J., Chen, X., Haigis, K., Jegga, A.G., *et al.* (2007). Transcriptional recapitulation and subversion of embryonic colon development by mouse colon tumor models and human colon cancer. *Genome Biol* 8, R131.

Kataoka, K., Noda, M., and Nishizawa, M. (1994). Maf nuclear oncoprotein recognizes sequences related to an AP-1 site and forms heterodimers with both Fos and Jun. *Mol Cell Biol* 14, 700-712.

Wang, Y., Cortez, D., Yazdi, P., Neff, N., Elledge, S.J., and Qin, J. (2000). BASC, a super complex of BRCA1-associated proteins involved in the recognition and repair of aberrant DNA structures. *Genes Dev* 14, 927-939.